Supplementary Material

Microstructure optimization strategy of $ZnIn_2S_4$/rGO composites toward enhanced and tunable electromagnetic wave absorption properties

Ran Xu[a], Man He[a,*], Shuangjiang Feng[a], Yanmei Liu[a], Chunfeng Mao[a], Yongjuan Wang[a], Xiaohai Bu[a,b,d], Meiyun Zhang[e], Yuming Zhou[a,c,*]

[a]School of Chemistry and Chemical Engineering, Southeast University, Jiangsu Optoelectronic Functional Materials and Engineering Laboratory, Nanjing 211189, China

[b]School of Materials Science and Engineering, Nanjing University of Science & Technology, Nanjing 211167, China

[c]Jiangsu Sidik New Material Technology Co., Ltd, Suqian 223900, China

[d]ZY fire Hose Co., Ltd, Taizhou 225599, China

[e]Key Laboratory of Auxiliary Chemistry and Technology for Chemical Industry, Ministry of Education, Shaanxi University of Science & Technology, Xi'an 710021, China

Material characterization:

The crystalline structure was identified by X-ray diffraction (XRD) with Cu Ka radiation in the scope of 5-80° (2θ). The characteristic vibrational modes were measured on a Bruker Tensor 27 FT-IR spectrometer. Raman spectra were gained by a Thermos Fisher Raman microscopy system (laser wavelength, 514 nm; spot size, 150 μm) in the wavenumber of 1000-2100 cm^{-1}. X-ray photoelectron spectroscopy (XPS, VG Scientific) was utilized to identify the compositions and chemical states of elements of samples. The morphologies of the samples were observed by field emission scanning electron microscope (FESEM, FEI Inspect F50) and transmission electron microscope (TEM). The specific surface areas and the pore size distributions of samples were detected by BET method (ASAP 2010, USA). The electromagnetic parameters of samples were tested by Agilent PNAN5244A vector network analyzer in the frequency range of 2-18 GHz in the light of the coaxial-line method. The measured samples were prepared by evenly compounding products with paraffin wax (the mass ratio is 0.3) and then casted into ring-shaped samples (Φout: 7.0 mm, Φin: 3.04 mm).

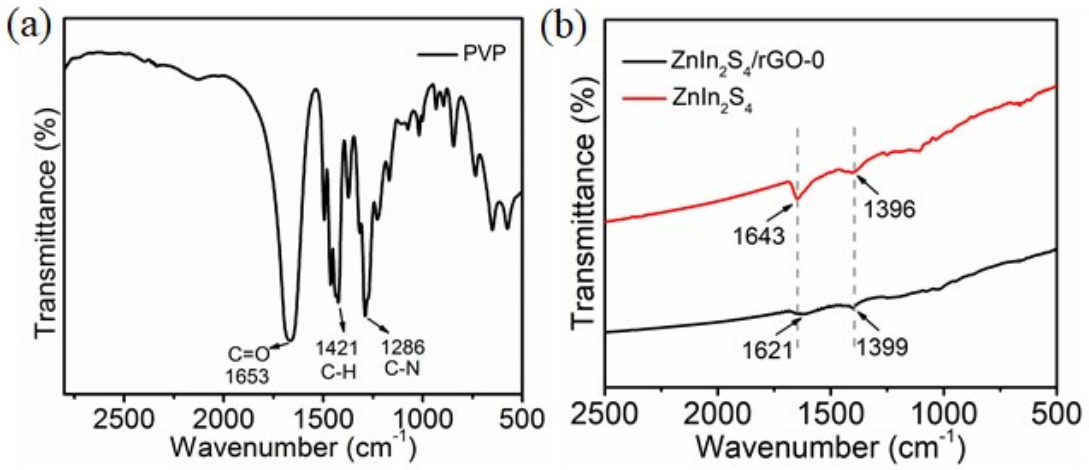

Fig. S1 FTIR spectra of (a) PVP, (b) as-prepared $ZnIn_2S_4$ and $ZnIn_2S_4$/rGO-0 composites.

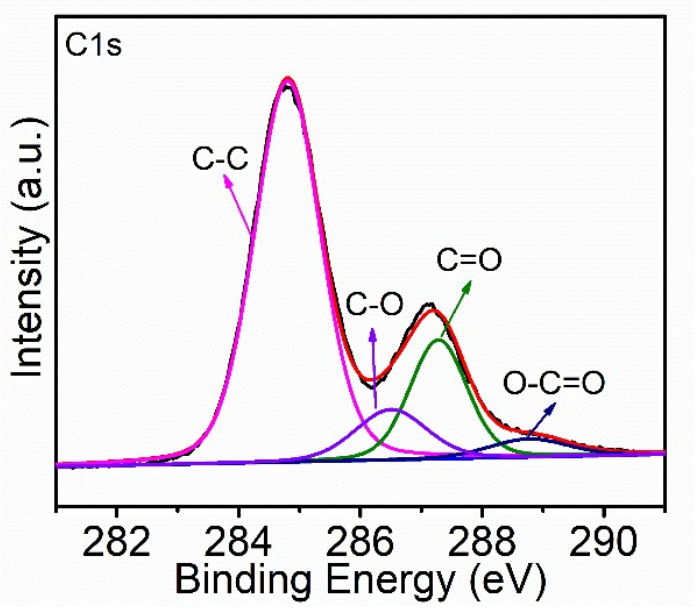

Fig. S2 XPS spectra in C1s region for GO.

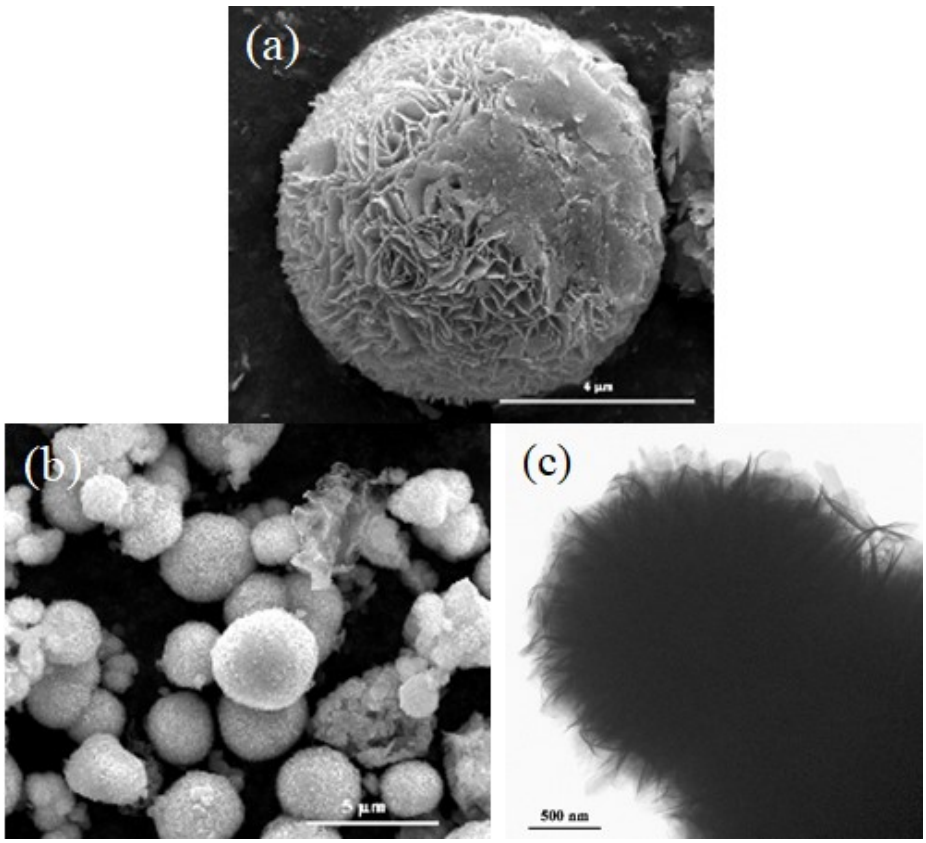

Fig. S3 SEM images of (a) bare $ZnIn_2S_4$, (b) $ZnIn_2S_4$/rGO-0 composites and TEM image of (c) $ZnIn_2S_4$/rGO-0 composites.

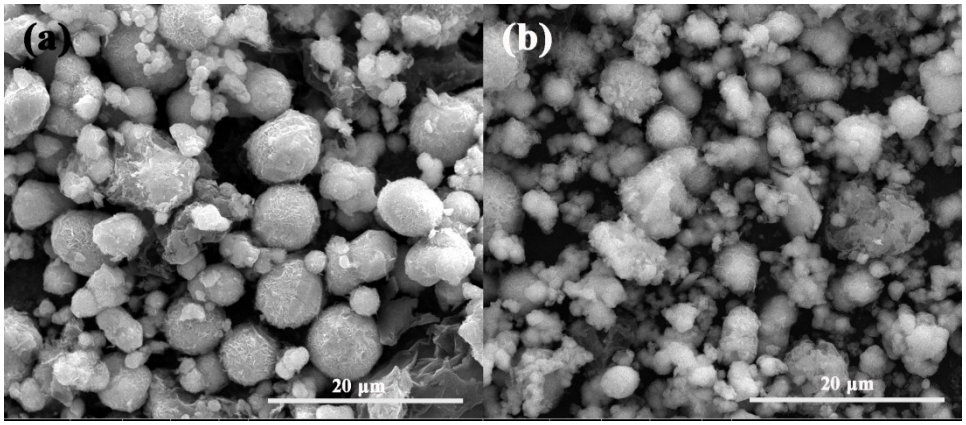

Fig. S4 Low-magnification SEM images of (a) $ZnIn_2S_4$/rGO-0, (b) $ZnIn_2S_4$/rGO-1 composites.

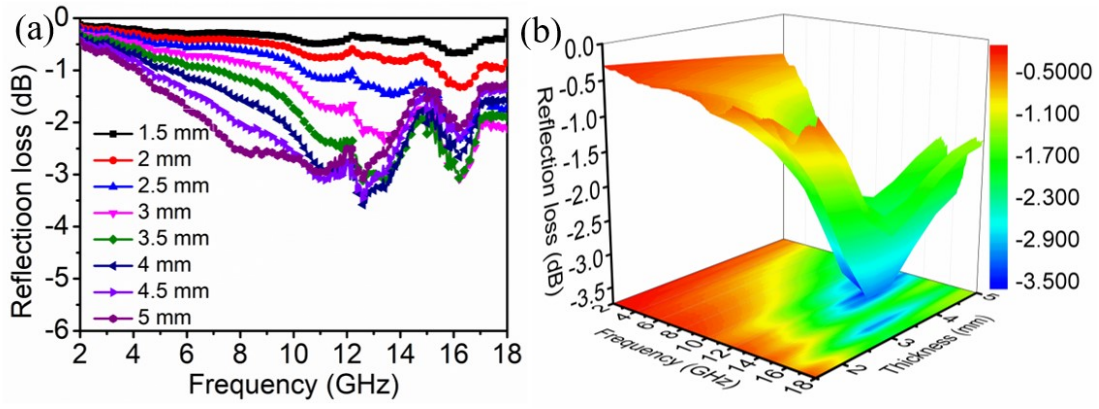

Fig. S5 (a) RL plots and and (b) 3D RL plots at the frequency range of 2-18 GHz: $ZnIn_2S_4$.

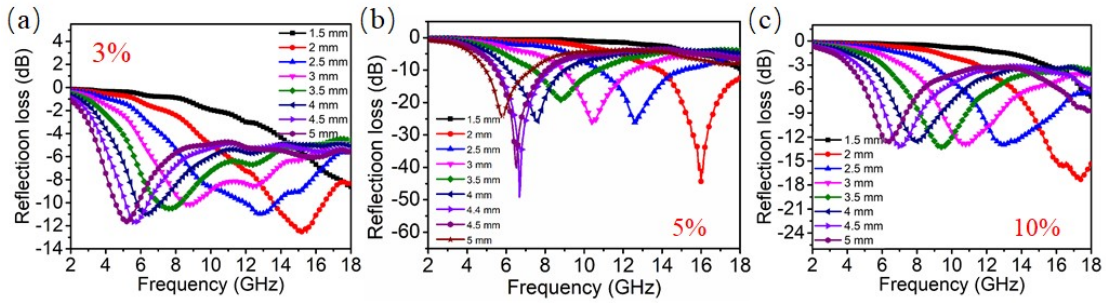

Fig. S6 Plotted RL curves at different thicknesses: (a) $ZnIn_2S_4$/rGO-3% composites; (b) $ZnIn_2S_4$/rGO-5% composites; (c) $ZnIn_2S_4$/rGO-10% composites. (The PVP contents of these composites keep at 0.1 g.)